Determination of the inductance of imploding wire array Z-pinches using measurements of load voltage

G. C. Burdiak, S. V. Lebedev, G. N. Hall, A. J. Harvey-Thompson,[a] F. Suzuki-Vidal, G. F. Swadling, E. Khoory, L. Pickworth, S. N. Bland, P. de Grouchy, and J. Skidmore
Blackett Laboratory, Imperial College, London SW7 2BW, United Kingdom

(Received 1 February 2013; accepted 22 February 2013; published online 12 March 2013)

The inductance of imploding cylindrical wire array z-pinches has been determined from measurements of load voltage and current. A thorough analysis method is presented that explains how the load voltage of interest is found from raw signals obtained using a resistive voltage divider. This method is applied to voltage data obtained during z-pinch experiments carried out on the MAGPIE facility (1.4 MA, 240 ns rise-time) in order to calculate the load inductance and thereafter the radial trajectory of the effective current sheath during the snowplough implosion. Voltage and current are monitored very close to the load, allowing these calculations to be carried out without the need for circuit modelling. Measurements give a convergence ratio for the current of between 3.1 and 5.7 at stagnation of the pinch. © *2013 American Institute of Physics*.
[http://dx.doi.org/10.1063/1.4794957]

I. INTRODUCTION

Simultaneous, independent measurements of z-pinch load voltage and current allow the electrical power being delivered to the load by the generator to be calculated. More specifically, these measurements allow for load resistance and resistive energy deposition to be determined, as well as load inductance and the associated energy stored in the magnetic field. This goes some way to calculating the energy balance of the complete z-pinch system, which will also include components from radiation and the kinetic energy of the dynamic plasma. Energy deposition and inductance measurements are very important for the understanding and design of many z-pinch loads. Such measurements have been carried out on cylindrical wire arrays,[1–6] gas-puffs,[7] inverse arrays,[8] and radial foil z-pinches.[9]

A new electrical probe for making z-pinch load voltage measurements has been designed, calibrated and fielded on the MAGPIE generator,[10] a 1.4 MA, 240 ns rise-time pulsed-power device at Imperial College London. The general expression for the voltage drop across a z-pinch load is the following:

$$V_{load}(t) = L(t)\frac{dI(t)}{dt} + I(t)\frac{dL(t)}{dt} + I(t)R(t). \qquad (1)$$

Note that the load inductance, L, and the load resistance, R, are in general time-dependant. The first two terms in Eq. (1) result from the rapidly changing magnetic flux threading the load/return post structure. For an imploding z-pinch load fielded on the MAGPIE generator these terms can reach over 100 kV each due to the fast-rising MAGPIE current ($\sim 5.5 \times 10^{12}$ A/s) and the rapidly changing geometry of the current path during the final implosion of a wire array. Voltage measurements that are sensitive to the first two terms allow one to calculate the inductance and instantaneous magnetic energy stored in the load ($LI^2/2$). The third term represents the resistive voltage drop across the load. Sensitivity to this term allows one to calculate the load resistance, energy deposition through Joule (resistive) heating ($\int I^2 R dt$) and the time of plasma formation. A voltage probe is required that is sensitive to all three voltage components. In addition, a suitable probe will have a fast response and be capable of resisting electrical breakdown upon application of a few hundred kV in an intense UV radiation environment.

In the context of this paper, voltage and current measurements are used to determine the load inductance and thereafter the effective radial trajectory of the current sheath in imploding cylindrical wire array z-pinch loads. Inductance measurements have been carried out previously on both the Z facility[2,4–6] (20 MA, 100 ns rise) at Sandia National Laboratories in the US and on the Angara-5-1 facility[3] (5 MA, 250 ns) in Russia. In previous cases, however, the load voltage and/or the load current were monitored at significant distances from the load itself. This can cause complications arising as a result of current losses in vacuum power feeds to the load, occurring between the point of voltage measurement and the load itself. In addition, the instant of resistive breakdown of the wires early on in the current pulse was not directly measured in previous work involving inductance measurements. This will have a subtle effect on inductance unfolds.

In experiments described in this paper, the voltage was monitored directly at the high voltage (HV) side of the wire array, removing the need for circuit modelling and the possibility of undiagnosed current losses. The determination of the true load voltage from the voltage on the probe is not trivial, and we therefore provide a thorough explanation of our analysis method. We note that voltage measurements obtained with a direct connection to the HV electrode of a gas puff z-pinch load on the Saturn generator at Sandia (6 MA, 300 ns rise) were described in Ref. 7. However, an analysis routine that properly takes into account the mutual

[a]Current address: Sandia National Laboratories, Albuquerque, New Mexico 87185-1106, USA.

inductance of the load and voltage probe current loops has not previously been described in sufficient detail.

The remainder of this paper is structured as follows: In Sec. II the design of a new resistive voltage divider is described, together with a test of its operation. In Sec. III we present general voltage characteristics of wire array implosions. In Sec. III A the analysis method used for determining load voltage and inductance is presented. Finally, in Sec. III B, trajectories for the radius of the current sheath during the final implosion of aluminium (Al) wire array loads are unfolded from inductance measurements and compared to implosion trajectories inferred from optical streak images. We find the time for the beginning of the implosion well correlated between electrical and optical streak diagnostics. We also find the average current convergence ratio to be between 3.1 and 5.7, poorer than the convergence of visibly radiating matter suggested by streak images.

II. DESIGN AND TESTING OF THE VOLTAGE DIVIDER

A. Design

The voltage probe was designed along the lines of a resistive/capacitive divider that was previously described by Pellinen[11] and later developed and fielded on the Saturn generator.[7] It operates under vacuum, very close to the z-pinch load, and is capable of functioning beyond the point of peak radiated power generated by the implosion. The probe consists of two stages of voltage division as shown in the diagram in Fig. 1. The first stage provides geometric division

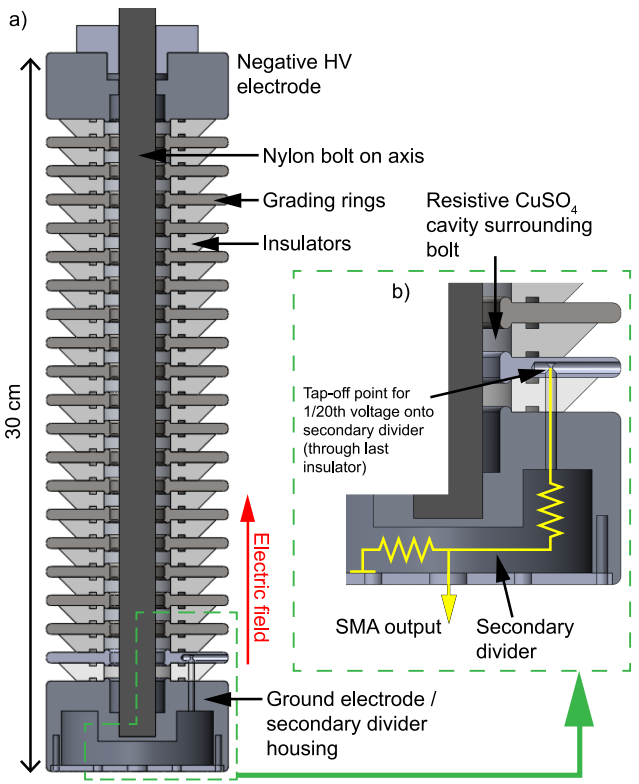

FIG. 1. (a) Section computer-aided design (CAD) image of the voltage probe showing the primary geometric division stack. (b) Enlarged section CAD image of the voltage probe, including a schematic for the secondary divider inside the ground electrode.

along a stack of alternating annular acrylic insulators and stainless steel grading rings that enclose a cavity filled with resistive copper sulphate solution. For this type of voltage divider, uniform field division should occur for all input frequencies. Therefore, recorded pulse shapes are not distorted by frequency filtering. The ~30 cm long stack is compressed with an axial nylon bolt. The resistance of the stack is ~400 Ω; this is much larger than the load resistance, typically no more than a few Ω in the present experiments, so current loading should be negligible. The voltage across the last stage of the primary column (1/20th of the total voltage across the length of the stack) is tapped off onto a secondary divider made from conventional solid state resistors. The series resistance of the secondary divider (~1 kΩ) is much greater than that of the last stage in the primary column (~20 Ω); this ensures that the exact concentration of the copper sulphate solution has a negligible effect on the final division ratio of the probe. The total attenuation factor for the combined stages of the probe is 1:1600. The rise-time of the probe has not been measured experimentally. However, it has been estimated from the probe geometry and through-resistance to be approximately $t_{rise} = 2.2RC \approx 1.3$ ns. This is adequate even for the short lived (~20 ns) resistive phase of wire array z-pinches fielded on the MAGPIE generator.

B. Test of voltage probe operation using a non-imploding load

The voltage probe attenuation was checked against Rogowski groove current monitors during a short circuit MAGPIE experiment. The short circuit load consisted of a solid, 8 mm diameter steel post, concentric with 4, evenly spaced current return posts, at a radius of 77.5 mm from the symmetry axis. The load has a constant inductance, L_{short}, as it cannot implode, and a very small resistance due to its large cross-sectional area and surface area. The voltage across the short is therefore given simply by

$$V_{short}(t) = L_{short}\frac{dI_{short}(t)}{dt}, \tag{2}$$

where I_{short} is the current through the axial load.

The voltage probe is sensitive to some fraction of V_{short}, dependant upon the amount of time-dependant magnetic flux that it samples: The HV connection of the probe with the load forms a current loop, and the size and position of the loop (essentially its inductance) determine the fraction of the total load voltage that is sampled by the probe. Rogowski groove current monitors, routinely fielded on current return posts during MAGPIE experiments, are only sensitive to dI/dt. The redundancy of these two diagnostics on this type of load was used to check the voltage probe attenuation. The Rogowski grooves have themselves been absolutely calibrated using a continuous-wave Faraday rotation diagnostic.[12]

The voltage probe was fielded vertically and end-on to the load as shown schematically in Fig. 2(a). Using this configuration, the magnetic flux threading the area shown in green could be calculated geometrically, assuming no magnetic flux exists above the level of the "top plate" in the

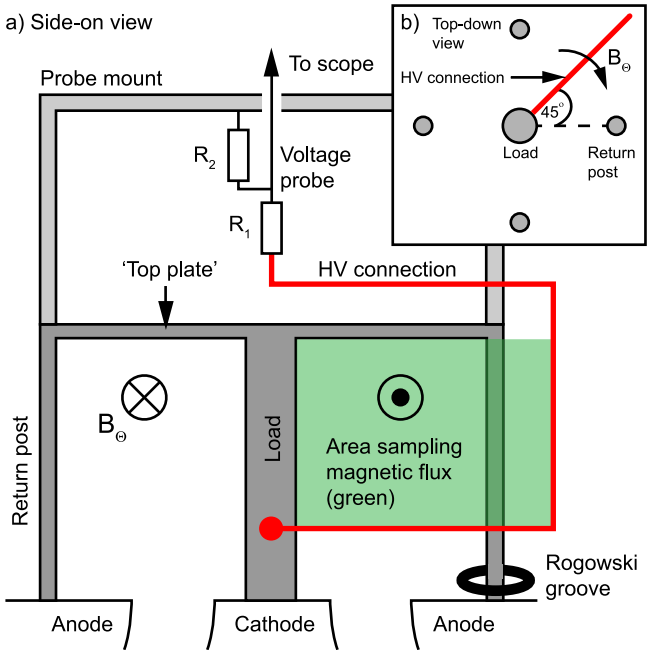

FIG. 2. (a) Side-on schematic for the fielding of the voltage probe during a short circuit calibration experiment. The voltage probe is fielded vertically and end-on to the load, supported by brass posts that connect to the "top plate" of the load hardware. Magnetic flux threading the green plane generates a voltage across the probe. (b) End-on schematic showing the orientation of the voltage probe connection relative to the current return posts.

figure. The magnetic flux threading the plane of the HV connection is purely azimuthal if the connection is made midway between two current return posts, as shown in Fig. 2(b). The radial distribution of the magnetic field was calculated using equations found in Ref. 13 for the field generated around arbitrary distributions of parallel conducting wires and includes contributions from all four return posts and the axial load. This field was used to calculate the inductance of the loop, L_{loop}. The ground electrode of the voltage probe was connected to the "top plate" of the load hardware, a position not strictly at ground. The coaxial cable from the probe to the vacuum chamber bulkhead was therefore given some inductance to prevent the outer conductor from drawing current. Two Rogowski groove probes were fielded on opposing (180° apart) return posts.

The voltage required to push the observed dI/dt, as measured by the Rogowski probes, through the theoretical inductance of the green loop in Fig. 2, was compared to the product of the raw voltage probe signal, V^{raw}_{probe}, and its theoretical calibration, C (where $C = 1600$). The results of this experiment are shown in Fig. 3. The voltage probe and Rogowski traces agree to within 10% until voltage reverses at ~280 ns. At this point the asymmetric insulating rings of the voltage probe become less effective; this could lead to breakdown and the corresponding divergence of the voltage probe and Rogowski signals.

III. LOAD VOLTAGE AND INDUCTANCE DURING CYLINDRICAL WIRE ARRAY IMPLOSIONS

The voltage probe has been fielded on cylindrical wire array loads for measurements of resistance and time-dependent

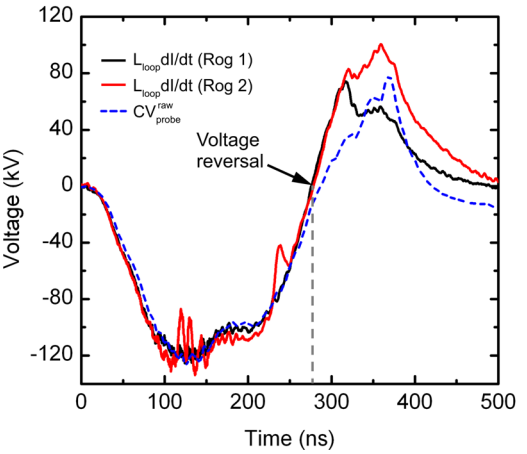

FIG. 3. Results from a cross calibration test between Rogowski grooves and the voltage probe. The voltage probe and Rogowski signals are in good agreement until voltage reversal (at 280 ns in this case).

load inductance. To measure the voltage during the implosion phase the probe is mounted side-on to the load with the high voltage electrode connected just below the array and the ground electrode bolted to the wall of the vacuum chamber, as shown schematically in Fig. 4(a) and in the photograph in Fig. 4(b). Note that both the voltage probe and Rogowski groove current monitors take measurements very close to the load; this is necessary to avoid having to use generator circuit models in the unfolding of raw signals, as was described in Refs. 2, 5, and 6. The line of sight from the pinch to the probe is blocked to protect against breakdown induced by UV photons from the load. With this arrangement, a combination of both the resistive voltage drop across the load *and* the time-dependant magnetic flux threading the green closed loop will generate a voltage across the probe. During these experiments, the standard MAGPIE diagnostics suite was also employed.

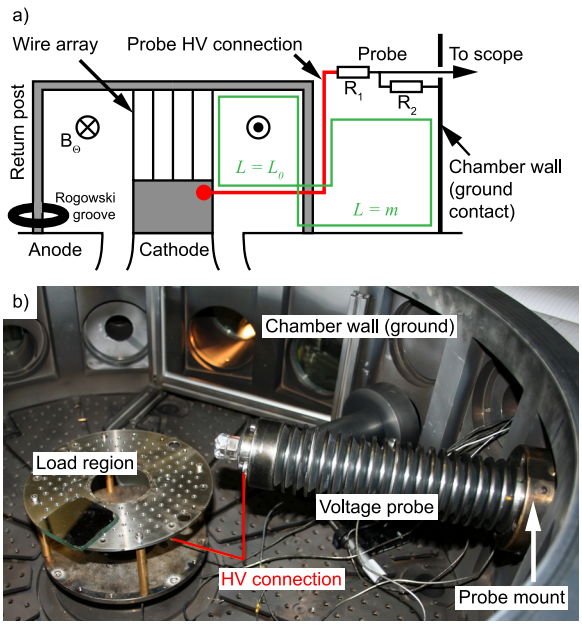

FIG. 4. (a) Schematic showing the complex nature of the voltage probe connection when fielded to monitor load voltage during the implosion of a wire array z-pinch. (b) Photograph of the voltage probe inside the MAGPIE load chamber.

This includes 2-frame, 532 nm laser probing (shadowgraphy, schlieren, and interferometry channels), an optical streak camera, 4-frame extreme ultraviolet (XUV) cameras, and a 5-channel diamond photo-conducting detector (PCD) pack.

Fig. 5 shows the typical voltage drop across a wire array load as measured by the voltage probe, along with the corresponding signal from a return post Rogowski groove. The Rogowski groove signal has been multiplied by L_0, the initial, geometric inductance of the array. There is a fast spike in the voltage signal at early times, superimposed on a slowly varying rise. This 20 ns, ~70 kV peak is attributed to increased resistance caused by Joule heating of the wires and subsequent breakdown upon plasma formation on the wire surface. We call this early time behaviour the *resistive phase* of the wire array implosion. The resistive voltage component, V_R, can be roughly separated from the total array voltage by subtracting $L_0 dI/dt$ from the total voltage trace. Using the peak resistive voltage and an accompanying current measurement (obtained by numerical integration of the Rogowski dI/dt signal), the peak resistance of this particular array ($4 \times 50\ \mu$m Al alloy 5056) is found to be $(1.4 \pm 0.2)\ \Omega$. Interestingly, this value is close to the resistance ($1.3\ \Omega$) of an array with the same dimensions, but with an average resistivity equal to that of pure Al at the boiling temperature, 2790 K. The amount of Joule heating occurring up to the time of peak resistance is estimated from the integral $\int IV_R dt$ (using measured current and voltage) to be 8–14 J. For comparison, the energy required to bulk heat the array mass to the vapour phase, at boiling temperature, is 6.2 J. Given that the wires are unlikely to be heated uniformly, we can say with some confidence that enough energy has been deposited for conducting plasma to be formed on the wire surface. The strong resistive signature in the array voltage therefore gives us an accurate measurement of the time for plasma formation. There is a relatively large error in the Joule heating measurement because the probe measures the total load voltage. It is not possible to separate the resistive voltage component from the inductive components with a high degree of accuracy. A more accurate method is to record only the resistive voltage component in the first instance. A suitable method for achieving this, at early times in the drive current pulse (before the implosion begins), is explained in Ref. 1, wherein load resistance and resistive heating are determined for wire arrays driven by the Angara-5-1 facility. Such measurements have also been carried out during MAGPIE experiments, using the same probe described in Sec. II A. These will be described in a future publication.

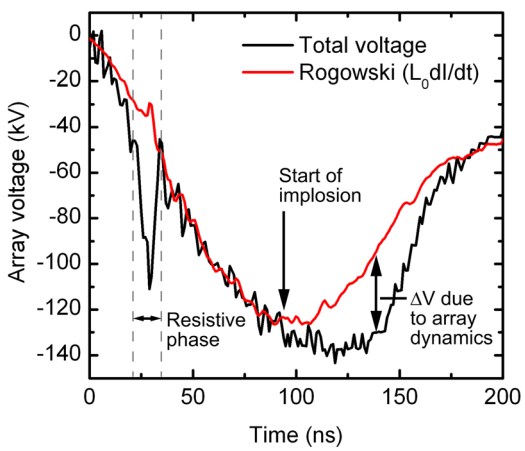

FIG. 5. Graph showing the typical voltage drop across a cylindrical wire array z-pinch. The black line shows the total load voltage. The red line shows the dI/dt component of the load voltage as measured by a return post Rogowski groove probe. The two signals differ during the resistive and implosion phases. The load consisted of $4 \times 50\ \mu$m Al wires, on an 8 mm radius. Shot number: s1214_09.

After breakdown of the wires and formation of plasma, the resistance will be negligible for a significant fraction of the implosion, and an inductive voltage drop dominates the signal. The slowly varying rise in the total voltage over the first ~100 ns of the current pulse is due to the large dI/dt from the generator. The shape of this part of the voltage signal follows the trace from the Rogowski groove, which is sensitive purely to dI/dt, both at the very beginning of the current pulse and after the end of the resistive phase. The total voltage waveform begins to deviate from the Rogowski waveform when plasma and current start to move towards the axis and hence the inductance becomes time-dependant. Upon the final implosion of the array ~1 MA of current begins to move radially inwards at $\sim 150\ \mathrm{km\,s^{-1}}$. Thus the dynamic voltage component, IdL/dt, becomes large, and the total voltage waveform deviates strongly from that of the Rogowski ($\propto dI/dt$) signal.

A. Analysis method for determination of load voltage and inductance

With a voltage probe signal and a pure dI/dt signal from a return post Rogowski probe, it is possible to reconstruct the inductance, $L(t)$, during the implosion of a wire array, and thus determine the bulk implosion trajectory of the current. In these experiments, this can be achieved without the need for circuit model analysis. The method for doing so is now described. To determine $L(t)$ we first need to determine the voltage drop associated purely with the load. We proceed by calculating the initial load inductance, L_0. Ignoring a small correction term, this is done using the following equation:

$$L_0 = L_{global} + L^{wires}_{private} + L^{returns}_{private} = \frac{\mu_0 l}{2\pi} \ln \frac{r_{return}}{r_{array}} + \frac{\mu_0 l}{2\pi} \frac{1}{N_w} \left[\ln \frac{r_{array}}{N_w r_{wires}} + 1 \right] + \frac{\mu_0 l}{2\pi} \frac{1}{N_{ret}} \left[\ln \frac{r_{return}}{N_{ret} r_{post}} + 1 \right], \tag{3}$$

where l is the array length, N_w is the number of wires, N_{ret} is the number of return posts, and the other variables are defined in Fig. 6. This equation has been modified from one found in Ref. 14 to include the effect of discrete return posts.

The probe will be sensitive to some fraction, f, of the magnetic flux that we are interested in. Due to the complex 3-dimensional nature of the voltage probe connection to the load, it is not possible to accurately calculate this fraction geometrically; instead, it is determined experimentally. In the following analysis, we assume that resistance is negligible for all times after the formation of plasma at the end of the resistive phase and remains so up to the point of peak

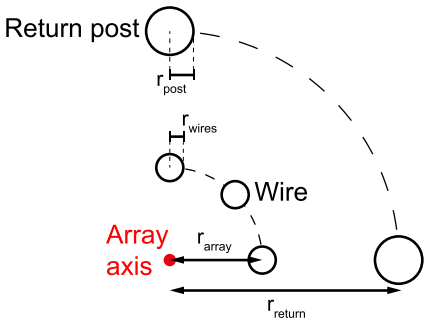

FIG. 6. Diagram explaining the terms used in Eq. (3) to calculate the initial array inductance.

radiated soft x-ray power. We note that this assumption may not be valid during and after the stagnation of the pinch.[5] With this assumption in mind, we can write the following for the measured voltage across the probe at times before the implosion begins (i.e., before $L = L(t)$):

$$V_{probe} = fL_0 \frac{dI}{dt}. \tag{4}$$

Referring to Fig. 4, this voltage will be due to the array inductance, L_0, and some extra inductance, characterised by m, caused by the precise way that the voltage probe is connected to the load hardware. Hence

$$V_{probe} = (L_0 + m)\frac{dI}{dt}, \tag{5}$$

and we can find m in terms of f

$$m = L_0(f - 1). \tag{6}$$

The fraction f is found by scaling the signal from the voltage probe to match that of the Rogowski at early times when $L(t) = L_0$. An example of this process is shown in Fig. 7. Here, the voltage probe signal is compared to $L_0 dI/dt$, where L_0 was calculated using Eq. (3), and dI/dt was measured with a Rogowski probe. In Fig. 7(b), the voltage probe signal has been multiplied by $1/f = 1.4$ to match $L_0 dI/dt$. For all times after resistive breakdown $(t > t_0)$ we can now write the following for the array voltage:

$$V_{array}(t) = V_{probe}(t) - m\frac{dI(t)}{dt}. \tag{7}$$

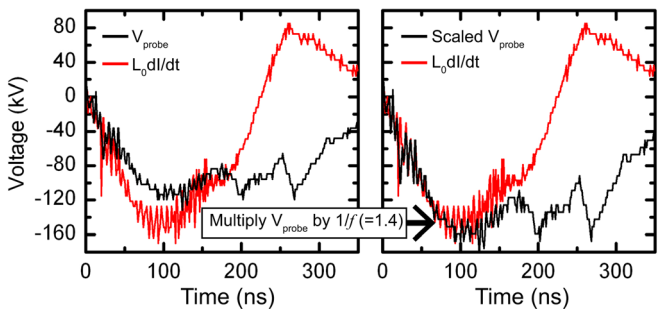

FIG. 7. Graphs showing the scaling procedure used to determine the inductance quantity, m, in Eq. (6). The voltage probe signal is matched to the Rogowski at early times, before implosion begins.

Equation (7) effectively corrects the voltage probe signal for any inductive pickup not directly associated with the load. Using the general formula $V = d(LI)/dt$, we can now write the following expression for the array inductance:

$$L(t) = \frac{1}{I(t)}\left[\int_{t_0}^{t} V_{array}(t)dt + I_0 L_0\right], \tag{8}$$

where the current $I(t)$ is found by integrating the Rogowski signal and I_0 is the current at the time of resistive breakdown.

The load voltage from a standard cylindrical array, calculated using the analysis method outlined above, is shown as the black line in Fig. 8. The red line shows the $L_0 dI/dt$ component of the total voltage, as measured by a Rogowski probe. The array was designed to stagnate close to peak current and consisted of $32 \times 15\,\mu$m Al wires, 20 mm long, on an 8 mm radius. The voltage probe functions through the point of peak x-ray power as indicated by the (uncalibrated) $2\,\mu$m polycarbonate-filtered PCD signal shown in green on the plot. Other generator diagnostics suggest that breakdown of the magnetically insulated transmission line[10] (MITL) occurred at the time indicated, causing the flat top to the Rogowski signal and the corresponding dip in the voltage probe signal. This does not affect the outcome of inductance analysis since both the Rogowski and voltage probes continue to monitor load voltages.

The inductance up to peak soft x-ray power, calculated using Eq. (8), is plotted as a solid blue line. The dashed line after this time shows a continuation of the calculation, ignoring possible effects of increased resistance after stagnation and potential breakdown of probes, etc. The calculation begins at the time of resistive breakdown of the wires, with the value of the initial array inductance, L_0, which was 16.2 nH for this particular load. The inductance of the array shows only a very modest increase during the first 180 ns (70%) of the implosion. This is consistent with the well established model for the ablation phase of a wire array implosion, during which the majority of the current flows in a hot, low density coronal

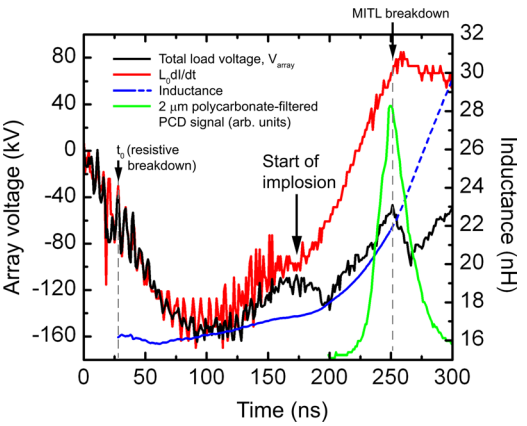

FIG. 8. (Black line) Wire array load voltage from current start to beyond peak radiated power. The temporal form of the soft x-ray pulse, as measured by a diamond photo-conducting detector, is shown by the green line. (Red line) dI/dt component of the load voltage with the initial inductance, L_0. (Blue line) Load inductance as determined by measured voltage signals, shown dashed after stagnation of the z-pinch. The load consisted of $32 \times 15\,\mu$m Al wires, on an 8 mm radius. Shot number: s1218_09.

plasma that surrounds stationary wire cores.[15] During this time, material continuously flows towards the axis in ablation streams that are fed by the coronal plasma. The slight increase in inductance over this period is consistent with a small amount of current being advected radially inwards with the flow of ablated plasma from the wires. Current advection during the ablation phase has been observed and discussed by the Cornell[16,17] and Angara[3,18] research groups, both of which used small B-dot probes to measure the presence and evolution of magnetic field inside the array radius. Thompson scattering measurements taken during the ablation phase of 8 mm radius, 32-wire Al arrays on the MAGPIE generator[19] show an increase in the ablation flow velocity from 5×10^6 cm s^{-1} at $0.7r_0$, to 1×10^7 cm s^{-1} at $0.2r_0$. This acceleration must indicate the presence of current and magnetic field inside the array radius. Previous work carried out on the MAGPIE facility indicates only a few percent of the total current flows in the ~1 mm radius precursor column on the axis. These measurements were based on techniques as diverse as stability analysis,[20] Faraday rotation,[21] and magnetic pickup.[22] Simulations[23] also show a distribution of the current inside the array at the beginning of the implosion phase, giving approximately 15% of the total current within half the initial array radius for 32-wire Al arrays. This number is in good agreement with Angara measurements.[18]

The array voltage begins to deviate strongly from $L_0 dI/dt$ approximately 180 ns into the implosion. Correspondingly, the inductance begins to increase more rapidly at this time. This point signifies the beginning of the snowplough implosion phase of the wire array,[24] during which a large fraction of the initial array mass, together with a large fraction of the total current, is swept radially inwards toward the axis by the $\mathbf{j} \times \mathbf{B}$ force. The divergence of the voltage signal from $L_0 dI/dt$ corresponds in time to the beginning of the implosion seen in optical streak images (see Fig. 10(a)).

B. Implosion trajectories from inductance measurements

Inductance measurements can be used to estimate an effective, average radius for the current in the pinch. One method for doing this is to model the implosion of the array as the convergence of a thin, cylindrically symmetric current sheath of radius $r(t)$. In the following analysis, the initial inductance of the imploding sheath is taken to be the value measured just before the onset of the main implosion and is denoted L_0^{imp}. We believe this is the most appropriate value to choose when setting the initial conditions for the implosion, which we further assume to be driven by 100% of the measured current pulse. The value of L_0^{imp} for the experiment in Fig. 8 was 17.3 nH. The time for the onset of the main implosion is taken as the time at which the gradient of the Rogowski dI/dt trace reverses with respect to the voltage probe trace (as indicated by the arrow in Fig. 8). The following expression for the ensuing change in load inductance can then be written down:

$$\Delta L = L(t) - L_0^{imp} \approx \frac{\mu_0 l}{2\pi} \ln\left(\frac{r_0}{r(t)}\right), \tag{9}$$

where r_0 is the initial array radius and l is the length of the imploding region. Equation (9) can be rearranged to give an expression for the current trajectory

$$r(t) = \frac{r_0}{\exp\left(\frac{\Delta L}{2l}\right)}, \tag{10}$$

where length scales are in cm and ΔL is in nH. The current trajectory for the array voltage in Fig. 8 is shown as the solid black line in Fig. 9(a). The time for stagnation of the array mass "on axis" is given by the position of the star symbol and is defined here as the point of peak soft x-ray power. The temporal profile of the soft x-ray pulse is shown as the green line. Note that the stagnation time is sometimes defined instead as the time at which a radial optical streak trajectory of the main implosion converges on the axis (this may involve a linear extrapolation of the trajectory as it approaches the axis). Streak trajectory convergence typically occurs approximately halfway through the rise of the soft x-ray pulse (see, e.g., Ref. 15). The radius of the effective current sheath at stagnation is 2.6 mm, giving a convergence ratio for the current of $C_R = r_{initial}/r_{final} = 3.1$. If, instead of using L_0^{imp} to calculate ΔL in Eq. (9), we use the calculated geometric value of the initial array inductance, L_0, then the radius of an effective current sheath from the end of the resistive phase to stagnation can also be calculated. These calculations begin to converge with calculations using L_0^{imp} as the final implosion progresses, and the choice of the initial inductance value becomes less important. Values for the final radius achieved by the current pinch are reduced by up to 25% if we choose L_0 over L_0^{imp}.

It is instructive to compare the trajectory of the current sheath to that of the imploding plasma as indicated by radial optical streak images. A streak image obtained during the same experiment as that just described is shown in Fig. 10(a). The slit aperture of the streak camera sampled the full diameter of the array, along ~1 mm of the array length. The leading and trailing boundaries of the bright optical emission caused by the main implosion provide a pair of implosion trajectories and were used to estimate the radial

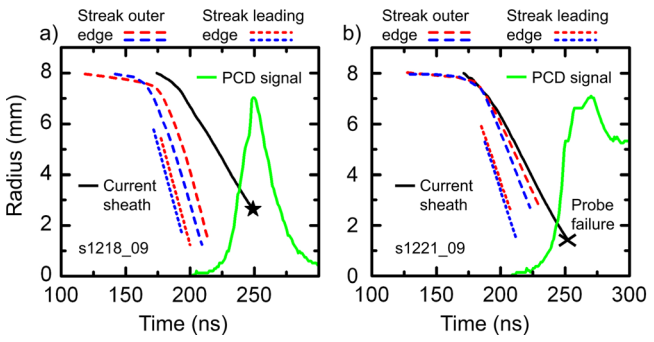

FIG. 9. Comparison of effective current sheath trajectories (as determined by voltage measurements) with optical streak implosion trajectories, for two nominally identical loads (32×15 μm Al). The outer and leading edges of the streak emission are plotted as long and short dashed lines, respectively. Streak trajectories either side of the array axis have been plotted in each case in red and blue. In plot (a) the voltage probe functions through stagnation (indicated by the star). In plot (b) the voltage probe fails at the point indicated by the cross, 18 ns before stagnation. The temporal profiles of the soft x-ray pulse produced in each experiment (as measured by a 2 μm polycarbonate-filtered diamond PCD) are given by the green lines.

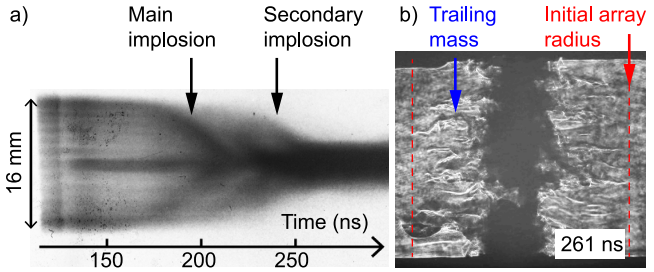

FIG. 10. (a) Optical streak image of a $32 \times 15\ \mu$m Al wire array implosion. The main implosion begins at ~180 ns, followed by a secondary implosion at ~230 ns. Shot number: s1218_09.

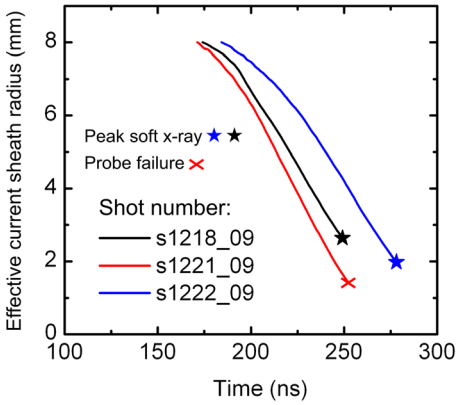

FIG. 11. Effective current sheath trajectories, calculated from voltage measurements, for three nominally identical loads ($32 \times 15\ \mu$m Al). In two experiments the voltage probe functions through stagnation (indicated by the star). In one experiment the voltage probe fails at the point indicated by the cross, 18 ns before stagnation.

evolution of the plasma accelerated by the magnetic piston. Two such pairs of trajectories (one pair from either side of the array axis) can be found from one streak image. Streak trajectories from Fig. 10(a) have been plotted as dashed-dotted lines in Fig. 9(a). Fig. 9(b) shows similar data from a nominally identical experiment. The current sheath trajectory calculation in Fig. 9(b) is terminated at 252 ns, 18 ns before stagnation, as the voltage probe failed at this point (most likely due to breakdown of the insulators, caused by UV flashover). The graphs in Fig. 9 clearly show that the beginning of the snowplough implosion phase correlates in time with the implosion of the current sheath. However, the emitting mass appears to propagate with a greater radial velocity, particularly in the experiment shown in Fig. 9(a), achieving a tighter convergence than the current at any given time. This result suggests that rather than pinching on axis during the main implosion, the current remains radially distributed, with much of it flowing in a lower inductance path at a greater radius than the emitting plasma participating in the main implosion might suggest. A large radius path for this current could be provided for by trailing mass that is left behind during the main implosion. This trailing mass is observed, for example, in laser shadowgraphy images such as the one shown in Fig. 10(b). Streak images also show emitting plasma left behind during the main implosion, which may pinch later in a secondary implosion (see Fig. 10(a)), driven by trailing current/magnetic field.[24]

It is evident from Fig. 9 that a different implosion trajectory is found from either side of one streak image. This is due to the complex 3D nature of the final implosion, which is magneto-Rayleigh-Taylor (MRT) unstable. The uncorrelated, randomised nature of the MRT bubbles and spikes around the circumference of the array means that the slit aperture of the streak camera will likely sample different implosion trajectories on opposite sides of the array axis. This effect may very well also explain the difference in the streak trajectories between the two experiments in Fig. 9. This clearly shows that an optical streak image obtained by sampling a ~1 mm section of the array length is not an ideal diagnostic for measuring implosion trajectories. Axially averaged streak images may produce more consistent results and provide more suitable information for comparison to electrical data.

Three current sheath implosion trajectories from nominally identical experiments are plotted together in Fig. 11 for comparison. In the two cases where the voltage probe functioned through peak radiated x-ray power, the effective convergence achieved at stagnation varied between $8/2.6 = 3.1$ (black line) and $8/2.0 = 4.0$ (blue line). In the case where the voltage probe failed, the convergence at stagnation must have been higher than $8/1.4 = 5.7$. Failure to account for resistance at stagnation means that these calculations should produce upper estimates for the current convergence. The numbers given are in rough agreement with those reported in Refs. 2 and 3 of ~6, for wire array implosions on the Z generator and Angara-5-1 facility, respectively. The shape of the current sheath trajectories is reasonably reproducible, and the differences observed are consistent with the slightly different drive currents measured in each case. The current convergence reached in these experiments is contrary to the size of the stagnation column indicated by XUV emission images of similar arrays,[22,25] which has a radius of 0.25–0.5 mm. Again, this is likely due to some fraction of the current flowing in a radially distributed manner through trailing mass, left behind after the main implosion.

IV. CONCLUSIONS

A new voltage divider has been fielded on MAGPIE-driven wire array z-pinch experiments to allow all components of the load voltage to be monitored, from current start through to stagnation and peak radiated x-ray power. The voltage probe and accompanying current monitors used in these experiments take measurements very close to the load, enabling load voltages to be determined without the need for circuit modelling to account for current losses in the MITL. The voltage monitor can be used to determine the load inductance, and as such it is a powerful diagnostic for evaluating the effectiveness of the current pinch during cylindrical wire array implosions. The effective radial convergence of the current path at stagnation in $32 \times 15\ \mu$m Al arrays was found to vary from 3.1 to 5.7 between nominally identical experiments. To this end, the voltage probe may further be used to study z-pinch loads with modified implosion dynamics, such as coiled arrays[26] and preconditioned arrays.[27] The voltage probe has also been used to study the early-time

resistive phase of wire array and liner z-pinches; these results will be presented in future publications.

ACKNOWLEDGMENTS

This work was supported by AWE Aldermaston, by EPSRC (Grant No. EP/G001324/1), and by the NNSA under DOE Cooperative Agreement Nos. DE-F03-02NA00057 and DE-SC-0001063.

[1]V. V. Aleksandrov, A. G. Alekseev, V. N. Amosov, M. M. Basko, G. S. Volkov, E. V. Grabovskii, A. V. Krasilnikov, G. M. Oleinik, I. N. Rastyagaev, P. V. Sasorov, A. A. Samokhin, V. P. Smirnov, and I. N. Frolov, "Experimental and numerical studies of plasma production in the initial stage of implosion of a cylindrical wire array," Plasma Phys. Rep. **29**, 1034–1040 (2003).

[2]E. M. Waisman, M. E. Cuneo, W. A. Stygar, R. W. Lemke, K. W. Struve, and T. C. Wagoner, "Wire array implosion characteristics from determination of load inductance on the z pulsed-power accelerator," Phys. Plasmas **11**(5), 2009–2013 (2004).

[3]V. V. Aleksandrov, E. V. Grabovskii, K. N. Mitrofanov, G. M. Oleinik, V. P. Smirnov, P. V. Sasorov, and I. N. Frolov, "Relation between the electric parameters of a z-pinch discharge and plasma production in the load during the implosion of a cylindrical wire array," Plasma Phys. Rep. **30**, 568–581 (2004).

[4]M. E. Cuneo, E. M. Waisman, S. V. Lebedev, J. P. Chittenden, W. A. Stygar, G. A. Chandler, R. A. Vesey, E. P. Yu, T. J. Nash, D. E. Bliss, G. S. Sarkisov, T. C. Wagoner, G. R. Bennett, D. B. Sinars, J. L. Porter, W. W. Simpson, L. E. Ruggles, D. F. Wenger, C. J. Garasi, B. V. Oliver, R. A. Aragon, W. E. Fowler, M. C. Hettrick, G. C. Idzorek, D. Johnson, K. Keller, S. E. Lazier, J. S. McGurn, T. A. Mehlhorn, T. Moore, D. S. Nielsen, J. Pyle, S. Speas, K. W. Struve, and J. A. Torres, "Characteristics and scaling of tungsten-wire-array *z*-pinch implosion dynamics at 20 ma," Phys. Rev. E **71**, 046406 (2005).

[5]E. M. Waisman, M. E. Cuneo, R. W. Lemke, D. B. Sinars, and W. A. Stygar, "Lower bounds for the kinetic energy and resistance of wire array z pinches on the z pulsed-power accelerator," Phys. Plasmas **15**(4), 042702 (2008).

[6]C. A. Jennings, M. E. Cuneo, E. M. Waisman, D. B. Sinars, D. J. Ampleford, G. R. Bennett, W. A. Stygar, and J. P. Chittenden, "Simulations of the implosion and stagnation of compact wire arrays," Phys. Plasmas **17**(9), 092703 (2010).

[7]D. P. Murphy, R. J. Allen, B. V. Weber, R. J. Commisso, J. P. Apruzese, D. G. Phipps, and D. Mosher, "Time-resolved voltage measurements of z-pinch radiation sources with a vacuum voltmeter," Rev. Sci. Instrum. **79**(10), 10E306 (2008).

[8]A. J. Harvey-Thompson, S. V. Lebedev, S. N. Bland, J. P. Chittenden, G. N. Hall, A. Marocchino, F. Suzuki-Vidal, S. C. Bott, J. B. A. Palmer, and C. Ning, "Quantitative analysis of plasma ablation using inverse wire array z pinches," Phys. Plasmas **16**(2), 022701 (2009).

[9]F. Suzuki-Vidal, S. V. Lebedev, S. N. Bland, G. N. Hall, G. Swadling, A. J. Harvey-Thompson, J. P. Chittenden, A. Marocchino, A. Ciardi, A. Frank, E. G. Blackman, and S. C. Bott, "Generation of episodic magnetically driven plasma jets in a radial foil z-pinch," Phys. Plasmas **17**(11), 112708 (2010).

[10]I. H. Mitchell, J. M. Bayley, J. P. Chittenden, J. F. Worley, A. E. Dangor, M. G. Haines, and P. Choi, "A high impedance mega-ampere generator for fiber z-pinch experiments," Rev. Sci. Instrum. **67**(4), 1533–1541 (1996).

[11]D. G. Pellinen and M. S. Di Capua, "Two-megavolt divider for pulsed high voltages in vacuum," Rev. Sci. Instrum. **51**(1), 70–73 (1980).

[12]G. F. Swadling, "An experimental investigation of the azimuthal structures formed during the ablation phase of wire array z-pinches," Ph.D. dissertation (Imperial College, London, 2012).

[13]F. S. Felber and N. Rostoker, "Kink and displacement instabilities in imploding wire arrays," Phys. Fluids **24**(6), 1049–1055 (1981).

[14]A. L. Velikovich, I. V. Sokolov, and A. A. Esaulov, "Perfectly conducting incompressible fluid model of a wire array implosion," Phys. Plasmas **9**(4), 1366–1380 (2002).

[15]S. V. Lebedev, F. N. Beg, S. N. Bland, J. P. Chittenden, A. E. Dangor, M. G. Haines, K. H. Kwek, S. A. Pikuz, and T. A. Shelkovenko, "Effect of discrete wires on the implosion dynamics of wire array z pinches," Phys. Plasmas **8**, 3734–3747 (2001).

[16]J. Greenly, M. Martin, I. Blesener, D. Chalenski, P. Knapp, and R. McBride, "The role of flux advection in the development of the ablation streams and precursors of wire array z-pinches," AIP Conf. Proc. **1088**(1), 53–56 (2009).

[17]M. R. Martin, C. E. Seyler, and J. B. Greenly, "The role of magnetic field in the transition to streaming ablation in wire arrays," Phys. Plasmas **17**(5), 052706 (2010).

[18]V. V. Aleksandrov, V. A. Barsuk, E. V. Grabovski, A. N. Gritsuk, G. G. Zukakishvili, S. F. Medovshchikov, K. N. Mitrofanov, G. M. Oleinik, and P. V. Sasorov, "Studies of penetration of the magnetic field into electrically imploded loads in the angara-5-1 facility," Plasma Phys. Rep. **35**, 200–221 (2009).

[19]A. J. Harvey-Thompson, S. V. Lebedev, S. Patankar, S. N. Bland, G. Burdiak, J. P. Chittenden, A. Colaitis, P. De Grouchy, H. W. Doyle, G. N. Hall, E. Khoory, M. Hohenberger, L. Pickworth, F. Suzuki-Vidal, R. A. Smith, J. Skidmore, L. Suttle, and G. F. Swadling, "Optical Thomson scattering measurements of plasma parameters in the ablation stage of wire array *z* pinches," Phys. Rev. Lett. **108**, 145002 (2012).

[20]S. C. Bott, S. V. Lebedev, D. J. Ampleford, S. N. Bland, J. P. Chittenden, A. Ciardi, M. G. Haines, C. Jennings, M. Sherlock, G. Hall, J. Rapley, F. N. Beg, and J. Palmer, "Dynamics of cylindrically converging precursor plasma flow in wire-array *z*-pinch experiments," Phys. Rev. E **74**, 046403 (2006).

[21]S. N. Bland, D. J. Ampleford, S. C. Bott, A. Guite, G. N. Hall, S. M. Hardy, S. V. Lebedev, P. Shardlow, A. Harvey-Thompson, F. Suzuki, and K. H. Kwek, "Use of faraday probing to estimate current distribution in wire array z pinches," Rev. Sci. Instrum. **77**(10), 10E315 (2006).

[22]S. V. Lebedev, D. J. Ampleford, S. N. Bland, S. C. Bott, J. P. Chittenden, J. Goyer, C. Jennings, M. G. Haines, G. N. Hall, D. A. Hammer, J. B. A. Palmer, S. A. Pikuz, T. A. Shelkovenko, and T. Christoudias, "Physics of wire array z-pinch implosions: Experiments at imperial college," Plasma Phys. Controlled Fusion **47**(5A), A91 (2005).

[23]J. P. Chittenden, S. V. Lebedev, B. V. Oliver, E. P. Yu, and M. E. Cuneo, "Equilibrium flow structures and scaling of implosion trajectories in wire array z pinches," Phys. Plasmas **11**(3), 1118–1127 (2004).

[24]S. V. Lebedev, F. N. Beg, S. N. Bland, J. P. Chittenden, A. E. Dangor, and M. G. Haines, "Snowplow-like behavior in the implosion phase of wire array z pinches," Phys. Plasmas **9**(5), 2293–2301 (2002).

[25]G. N. Hall, S. A. Pikuz, T. A. Shelkovenko, S. N. Bland, S. V. Lebedev, D. J. Ampleford, J. B. A. Palmer, S. C. Bott, J. Rapley, J. P. Chittenden, and J. P. Apruzese, "Structure of stagnated plasma in aluminum wire array z pinches," Phys. Plasmas **13**(8), 082701 (2006).

[26]G. N. Hall, J. P. Chittenden, S. N. Bland, S. V. Lebedev, S. C. Bott, C. Jennings, J. B. A. Palmer, and F. Suzuki-Vidal, "Modifying wire-array *z*-pinch ablation structure using coiled arrays," Phys. Rev. Lett. **100**, 065003 (2008).

[27]A. J. Harvey-Thompson, S. V. Lebedev, G. Burdiak, E. M. Waisman, G. N. Hall, F. Suzuki-Vidal, S. N. Bland, J. P. Chittenden, P. De Grouchy, E. Khoory, L. Pickworth, J. Skidmore, and G. Swadling, "Suppression of the ablation phase in wire array z pinches using a tailored current prepulse," Phys. Rev. Lett. **106**, 205002 (2011).